The Journal of Chemical Physics

Dispersive x-ray absorption spectroscopy for time-resolved *in situ* monitoring of mechanochemical reactions

Cite as: J. Chem. Phys. **157**, 214202 (2022); https://doi.org/10.1063/5.0130673
Submitted: 13 October 2022 • Accepted: 07 November 2022 • Accepted Manuscript Online: 08 November 2022 • Published Online: 01 December 2022

Published open access through an agreement with University of Birmingham School of Chemistry

Ana Guilherme Buzanich, C. Tufan Cakir, Martin Radtke, et al.

The Journal of Chemical Physics ARTICLE scitation.org/journal/jcp

Dispersive x-ray absorption spectroscopy for time-resolved *in situ* monitoring of mechanochemical reactions

Cite as: J. Chem. Phys. 157, 214202 (2022); doi: 10.1063/5.0130673
Submitted: 13 October 2022 • Accepted: 7 November 2022 •
Published Online: 1 December 2022

Ana Guilherme Buzanich,[1,a] C. Tufan Cakir,[1] Martin Radtke,[1] M. Bilal Haider,[1] Franziska Emmerling,[1] Paulo F. M. de Oliveira,[2] and Adam A. L. Michalchuk[3,a),b)]

AFFILIATIONS

[1] Federal Institute for Materials Research and Testing (BAM), Richard-Willstätter-Str. 11, 12489 Berlin, Germany
[2] Instituto de Química, Universidade de São Paulo, Av. Lineu Prestes 748, 05508000 São Paulo, Brazil
[3] School of Chemistry, University of Birmingham, Birmingham B15 2TT, United Kingdom

Note: This paper is part of the JCP Special Topic on *In situ* and Operando Characterization.
a) **Authors to whom correspondence should be addressed:** ana.buzanich@bam.de and a.a.l.michalchuk@bham.ac.uk.
b) **Also at:** Federal Institute for Materials Research and Testing (BAM), Richard-Willstätter-Str. 11, 12489, Berlin, Germany.

ABSTRACT

X-ray absorption spectroscopy (XAS) provides a unique, atom-specific tool to probe the electronic structure of solids. By surmounting long-held limitations of powder-based XAS using a dynamically averaged powder in a Resonant Acoustic Mixer (RAM), we demonstrate how time-resolved *in situ* (TRIS) XAS provides unprecedented detail of mechanochemical synthesis. The use of a custom-designed dispersive XAS (DXAS) setup allows us to increase the time resolution over existing fluorescence measurements from ~15 min to 2 s for a complete absorption spectrum. Hence, we here establish TRIS-XAS as a viable method for studying mechanochemical reactions and sampling reaction kinetics. The generality of our approach is demonstrated through RAM-induced (i) bottom-up Au nanoparticle mechanosynthesis and (ii) the synthesis of a prototypical metal organic framework, ZIF-8. Moreover, we demonstrate that our approach also works with the addition of a stainless steel milling ball, opening the door to using TRIS-DXAS for following conventional ball milling reactions. We expect that our TRIS-DXAS approach will become an essential part of the mechanochemical tool box.

I. INTRODUCTION

Despite over a century of research, the mechanisms that underpin mechanically induced chemical and physical transformations in and between solids (mechanochemistry) remain poorly understood.[1] To a large extent, this lack of understanding stems from the inherent difficulty of studying mechanochemical reactions. Inherently, mechanochemical reactions occur out of equilibrium,[2] making routine *ex situ* analysis a challenge. For example, mixtures of mechanically treated powders often evolve when aged at a finite temperature, even after the mechanical action has stopped.[3] In some cases, *ex situ* analysis has even provided seemingly erroneous interpretations of mechanochemical transformations.[4,5] To circumvent this challenge, growing efforts have focused on the development of time-resolved *in situ* (TRIS) technologies, able to monitor mechanochemical reactions during the mechanical treatment.[6,7] These developments have opened a new paradigm in mechanochemical research and have led to unique insights regarding mechanochemical reaction pathways[8,9] and the macrokinetics of mechanosynthesis.[5]

Various tools have already been developed for TRIS monitoring of mechanochemical reactions,[6,7,10] including synchrotron-based x-ray powder diffraction (XRD),[11,36] Raman spectroscopy,[12–14] thermometry,[15,16] solid-state nuclear magnetic resonance (NMR),[17]

acoustic emission,[18] and manometric measurements.[19,20] These various TRIS methods have proven powerful for studying bulk transformations at the crystallographic and molecular levels.

Existing methods focus primarily on bulk nuclear structure (molecular or crystallographic structure) or are indirect probes for the conditions within the milling jar. However, many important chemical and physical transformations involve changes in the electronic structure of the material. There are not yet any robust techniques available to monitor this characteristic of a mechanochemical transformation, representing a significant gap in experimental capabilities.[6,10] We have recently demonstrated a proof-of-concept that synchrotron-based x-ray absorption spectroscopy (XAS) can in principle be used to follow a ball milling reaction.[21] Unlike other available TRIS techniques, XAS offers an atom-sensitive probe to follow the evolution of the electronic structure of molecules and materials during mechanochemical treatment. Development of TRIS-XAS therefore promises to be an exciting addition to the mechanochemical toolbox.

In our proof-of-concept work using TRIS-XAS, we followed the redox processes involved in the bottom-up mechanochemical synthesis of Au nanoparticles.[21] Using a standard spectrometer setup required us to scan the incident energy, limiting the temporal resolution. Moreover, the intrinsic inhomogeneity of powder materials, coupled with the presence of a milling ball, only allowed for measurements in fluorescence mode and thus long acquisition times. These features severely limited the time resolution of the experiment, which required ~15 min per XANES spectrum at the Au L_3-edge (11.919 keV) to reach a suitable spectral quality. As such, setups using standard x-ray absorption near-edge structure (XANES) spectrometers do not meet the needs of the mechanochemical community.

Following from our previous success monitoring solution-phase reactions,[22] an energy dispersive setup [dispersive-XAS; dispersive x-ray absorption spectroscopy (DXAS)] seems to be a promising alternative for TRIS-XANES. In this approach, a polychromatic beam is used to excite the sample over a large area (typically 8 × 2 mm^2). The transmitted beam is dispersed by a convexly bent analyzer crystal [e.g., Si(111)], spatially resolving the energies to generate the XAS spectrum in a single "shot." This is collected by area-sensitive detectors, e.g., CCD-based. To date, this approach has been widely used to study the temporal dynamics of solutions, for example, in catalysis and corrosion.[22,23] However, because the spectrum is spatially resolved, one must ensure an exceptional degree of homogeneity across the probed sample. DXAS has therefore not been applied to the study of polycrystalline powders or solid mixtures.

In an attempt to minimize the inhomogeneity of a powder sample, we opted to follow mechanochemical reactions under resonant acoustic mixing (RAM) conditions. The RAM uses a low-frequency acoustic field (~60 Hz) to agitate the sample. In doing so, the RAM generates local mixing zones in the sample that are able to drive reactions in powder mixtures.[24–26] Encouraged by the high degree of powder mixing caused by the RAM, we explore for the first time the potential of DXAS as a tool for TRIS investigation of mechanochemically reacting powders. By focusing on RAM, we complement the only currently reported TRIS study of RAM kinetics[25] and provide additional evidence for the effects of different RAM conditions on the kinetics and efficacy of the reaction. In doing so, we demonstrate decisively that TRIS-DXAS is an exciting and complementary tool for studying mechanochemical reactions. We have demonstrated the generality of this new approach using two model systems: bottom-up metal nanoparticle synthesis and the mechanochemical synthesis of a prototypical metal–organic framework (MOF).

II. EXPERIMENTAL DETAILS

A. Materials and reactions

Materials were purchased from standard suppliers and used without further purification. The bottom-up mechanochemical synthesis of Au nanoparticles was done using the procedure outlined in Ref. 21, using Au^{III} ($HAuCl_4 \cdot 3H_2O$, 99.9%, Sigma-Aldrich; 101 mg) as a metal precursor, sodium borohydride ($NaBH_4$, 98%, Fischer Chemical; 20 mg) as the reducing agent, and polyvinylpyrrolidone (PVP; $\overline{Mw}$ = 10 000 g mol^{-1}, Sigma-Aldrich; 175 mg) as stabilizing agent. The synthesis of ZIF-8 was done from zinc oxide (112 mg), 2-methylimidazole (207.3 mg), using 50 μL of methanol and 20 mg of NH_4NO_3.

B. Resonant acoustic mixing

Reactions were performed using a Resodyn LabRAM I from Resodyn Acoustic Mixers. Reactions were performed in custom-designed Teflon (polytetrafluoroethylene, PTFE) jars with Kapton (polyimide) windows. The jars were 12 mm in internal diameter by 30 mm in internal height, with hemispherical bases. For each reaction, a total powder mass of ~300–350 mg was added to the jar. Reactions were performed at different accelerations (from 60 to 100 g; g = 9.8 m s^{-2}), with and without the addition of a 3 mm stainless steel ball, as outlined in the main text. While PTFE jars were used to minimize powder caking, the soft material may be damaged by the milling ball, though no macroscopic evidence was seen. Further development of jars made of stronger material (e.g., stainless steel) is ongoing.

C. Time-resolved *in situ* (TRIS) dispersive x-ray absorption spectroscopy (DXAS)

TRIS-DXAS measurements were performed at the BAM*line*, mounted on a 7 Tesla wavelength shifter at the BESSY-II storage ring (Helmholtz Center Berlin; HZB), Fig. 1. A polychromatic beam was selected based on the available optical stripes at the BAM*line*, Table I. For this study, we used either a broadband W/Si multilayer or a Pd mirror. The former provides incident energies of $E \pm 3.5\%$, sufficient for near-edge spectroscopy (XANES). The latter reflects a much broader range of energies (pink beam). The beam (8 × 2 mm^2) passes through our sample jar via the Kapton windows, Sec. II B. The setup uses a standard $\theta - 2\theta$ geometry, which simultaneously fulfills the entire energy range we wish to acquire, see Sec. III A. The transmitted beam is dispersed by an in-line convexly bent Si(111) crystal analyzer (Siegert Wafer GmbH (Aachen, Germany); thickness 525 μm, diameter 100 mm), which sits at an angle θ with respect to the incident beam. The dispersed beam is in turn captured by a fluorescence screen [P43 from ProxiVision GmbH (Bensheim, Germany)], which converts the x rays to visible light, placed at 2θ to the incident beam. The fluorescence screen is placed in front of a mirror objective [Rodenstock objective (Qioptiq

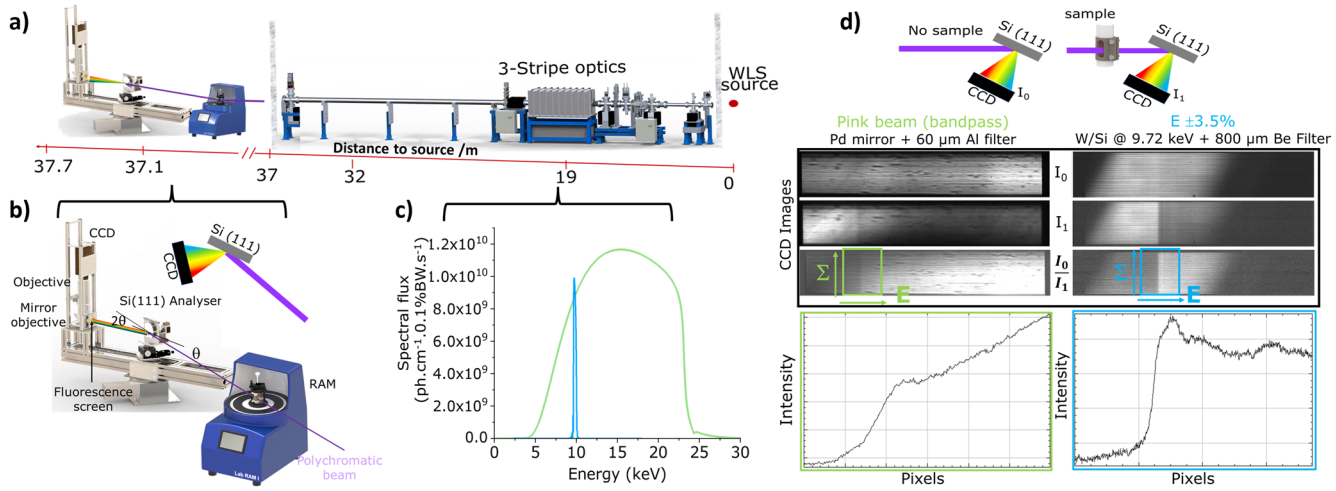

FIG. 1. Setup for TRIS-DXAS at the BAM*line*, mounted on a 7 T wavelength shifter (WLS) at BESSY-II. (a) The experimental setup for TRIS-DAXS shows the optical hutch with the three-stripe multilayer monochromator and the experimental hutch with the RAM and crystal detector setup. (b) A detailed view of the experimental setup showing the relative positions of the RAM, the Si(111) crystal analyzer, and the detector system. The Si(111) crystal analyzer is set at θ, and the detector system is set at 2θ to allow energy to be spatially resolved using Bragg scattering. (c) The incident spectral profiles for the Pd mirror (green) and the W/Si multilayer monochromator (blue), which are used for the Au and ZIF-8 reactions, respectively. (d) A schematic of the data collection for the spectral flux of the bare beam I_0 and the sample I_1, alongside images captured by the CCD detector for the spectral flux in the setup for the Au (left) and ZIF-8 (right) reactions. Note that the final spectra are obtained by the ratio I_1/I_0, as shown. Further details are given in Appendix B.

Photonic GmbH & Co. KG, Feldkirchen, Germany) with a focal distance of 100 mm], and further guided through a second objective [Nikon objective (Nikon Instruments Europe B.V., Amsterdam, Netherlands) with a focal distance of 180 mm] directed toward the CCD [pco.4000; PCO AG (Kelheim, Germany)]. Our CCD has a resolution of 4008 × 2672 pixels with a pixel size of $9 \times 9\ \mu m^2$. Together with the focal distances from both objectives, the pixel size of the recorded images is 4.8 μm. This allows a useable sensitive area of $19.46 \times 12.83\ mm^2$.

D. Data analysis

Data were processed and analyzed according to conventional methods using the open source software Larch.[27] Details are given in Appendix B. Quantitative analysis was achieved through least squares (LS) fitting as implemented within the Larch software. LS fits were performed using standard samples, measured in conventional transmission geometry: Au(0)- (Au(0) foil, Alfa Aesar); Au(I) - (AuCl, 99.9%, Sigma-Aldrich); Au(III)- ($HAuCl_4 \cdot 3H_2O$); ZIF-8; ZnO. See Appendix A for spectra.

III. RESULTS AND DISCUSSION

A. Developing the TRIS-DXAS setup for TRIS monitoring

The three-stripe optics, Fig. 1 and Table I, installed at the BAM*line* offers various routes for performing DXAS measurements. The Pd mirror, which provides total reflectance of the primary beam, could, in principle, be used for all DXAS measurements. However, in practice, the associated high photon fluxes combined with the width of the spectral range lead to significant damage to the sample. Instead, the broadband W/Si multilayer monochromator is well suited for most DXAS measurements where the XANES (near edge) region is of interest. This W/Si multilayer provides a 3.5% bandwidth around the target energy, which is usually sufficient to cover the

TABLE I. Construction of the three-stripe optics installed at the BAM*line*.

Stripe	1	2	3
Coating	Pd	W/Si	Mo/B_4C
Structure	Single	Periodic stripes	Periodic stripes
Layer thickness	39 nm	3.3 nm	2.8 nm
Energy range	Total reflection	6–10 keV 20–69 keV	6–20 keV <25 keV
Bandwidth (FWHM)	⋯	3.5%	1.2%

XANES region. In contrast, the Mo/B_4C multilayer monochromater offers a more narrow bandwidth, generally making it unsuitable for XANES.

From these technical considerations, our TRIS studies of ZIF-8 mechanosynthesis, Sec. III C, were done using the intrinsic 3.5% energy bandwidth of the W/Si multilayer at a central energy of 9.72 keV. This allowed us to capture a spectral range of ~9.38–10.07 keV. Unfortunately, problems arose with this approach when attempting to follow the RAM-driven Au nanoparticle synthesis. The Au L_3 edge is at 11.919 keV, which rests in the middle of the W $L_{1,2,3}$ edges, occurring at 12.1, 11.5, and 10.2 keV. Hence, when the W/Si multilayer is used for monitoring Au L_3, there is strong absorption from these W lines convoluted in the spectrum.

The incident beam profile for both of the experimental configurations used in this work, alongside the corresponding spectral flux for each configuration, is shown in Fig. 1. In both cases, the transmitted beam is dispersed from a convexly bent Si(111) single crystal analyzer, which is placed after the sample to minimize the detection of other scattering contributions (e.g., Bragg scattering). The dispersed beam is then detected using a fluorescence screen, which converts the x rays into visible light to be measured by a CCD, Fig. 1. In combination with objective lenses, see Sec. II, our setup detects the dispersed beam on the CCD over an area of 19.46×12.83 mm^2, black strips in Fig. 1. As the energy is resolved on the CCD in the horizontal axis, pixels in the vertical axis can be summed to enhance the final quality of the DXAS spectrum. The setup is aligned once for the required absorption edge, and all subsequent measurements are then performed without the need for further scanning of optics or monochromators,[28] thereby greatly increasing the rate of data collection over conventional spectrometers, which require monochromatic incident beams and hence scanning the monochromator.

As the spatial partitioning of energy follows Bragg conditions, the energy detected at any lateral position on the CCD depends on the scattering angle, θ. Consequently, with an incident beam of width BW, the detectable energy range and resolution across the illuminated length of the CCD, A_{CCD}, depend on the distance, L, between the Si(111) analyzer crystals and the fluorescence screen, such that the total range of energies ($\delta\theta$) captured on the CCD follows:

$$\delta\theta = \arctan\left(\frac{A_{CCD} - BW}{2 \times L}\right). \quad (1)$$

The experimental values in Eq. (1) used in this study are outlined in Table II, with the resulting CCD images shown in Fig. 1(c). In practice, the overall energy resolution at the CCD is a convolution of the bending radius of the crystal analyzer, the values of L and A_{CCD}, the focus of the lenses, and the pixel size of the CCD. The total spatial resolution achievable in our setup is at best 4.8 μm, with details provided in Sec. II. The final CCD image is converted to an energy axis by calibration to well-known metal foil standards, with typical calibrations performed in steps of 10 eV, Appendix B.

B. Bottom-up mechanochemical synthesis (BUMS) of Au nanoparticles (NP)

The mechanochemical synthesis of Au NPs has sparked considerable interest, particularly in terms of understanding formation mechanisms and learning to control the structure of the resulting NPs.[29–34] To this end, studies aimed at probing Au NP BUMS in real time are of particular interest. We have previously demonstrated that Au L_3-edge TRIS-XAS can in principle be used to follow the reduction of $HAuCl_4$ to form Au NPs during ball milling.[21] In our previous work, which used a standard spectroscopic (fluorescence) setup, a time resolution better than ~10–15 min was not possible. This greatly limited our ability to follow mechanochemical transformations or obtain macro-kinetic information. As a proof of concept for our new TRIS-DXAS setup, we therefore reconsider this Au NP BUMS process, Fig. 2. In comparison to our earlier work, our TRIS-DXAS setup provides a remarkable increase in time resolution, capable of measuring an entire XANES spectrum in only 2 s. We note, however, that the BUMS reaction proved to be very slow. We therefore opted to sum three datasets to minimize data analysis (i.e., giving an effective time resolution of 6 s). Without the presence of hard milling media, the hygroscopic reaction mixture for the BUMS-Au-NP synthesis quickly caked in the reaction vessel. This had the unfortunate effect of allowing us to monitor the reaction for only a short period of time (~30 min), and thus not to the completion of the reaction. However, we stress that, while unfortunate, this complication does not inhibit us from demonstrating the potential of TRIS-DXAS for mechanochemical reaction monitoring.

Our initial qualitative analysis clearly indicated the progressive, albeit slow, reduction of Au^{III} in response to RAM, Fig. 2. This is consistent with the reaction performed by ball milling.[21,31] With the high quality data obtained from our setup, we could additionally extract quantitative information regarding the RAM-driven BUMS processes using least squares fitting (Appendix B) to standard XAS spectra for $HAuCl_4 \cdot 3H_2O$, Au^I, and Au(0); see Appendix A. Hence, TRIS-DXAS can provide kinetic information at the scale of individual atoms without being restricted to the observation of crystalline materials such as TRIS-XRD. Although caking of the hygroscopic powder limited our reaction time to only ~30 min, quantitative analysis of the large number of spectral data still allowed us to identify some intriguing features of the RAM-driven BUMS process. Quantitative analysis shows very clearly that Au^{III} is reduced very gradually with continued RAM treatment, Fig. 2. Remarkably, our TRIS-DXAS data suggest that the BUMS of Au NP under RAM conditions proceeds via a different mechanism than under ball milling conditions. While ball-milling BUMS led to the formation of Au(0), no signs of the metallic state were observed in the first 30 minutes of RAM. Instead, there is a marked accumulation of the highly metastable Au^I species, indicating that RAM may provide a route to trapping this uncommon Au state. This will be the subject of dedicated follow-up investigations. The potential to detect Au^I under RAM conditions is quite remarkable. While it is well accepted that the formation of metallic Au from Au^{III} must pass via Au^I, only rare direct evidence of this mechanism has been reported.[35] It therefore appears that the gentle solid-state synthesis strategy possible by RAM may allow an exciting opportunity to elucidate new details of Au reduction.

In addition to the reduction of Au^{III} to Au^I, the high temporal resolution suggests marked inhomogeneity in the reaction volume, as evidenced by the fluctuating observation of Au^{III} and reduced Au species, Fig. 2. This is presumably due to the highly hygroscopic nature of the starting $HAuCl_4 \cdot 3H_2O$ species, which leads to the

TABLE II. Experimental setup for the TRIS DXAS spectrometer used in this work, with values tabulated for Eq. (1). The absorption edge is given alongside the configuration of the incident beam I_0, Fig. 1, the scattering angles θ, the Si(111) bending curvature (r_{bend}), the analyzer-detector distance (L), and the illuminated length of the CCD camera (A_{CCD}).

Experiment	Au	Zn
Abs. Edge/keV	11.919	9.659
I_0	Pd + 60 μm Al filter	W/Si @ 9.72 keV + 800 μm Be filter
$\theta/2\theta/°$	11.88/23.25	9.52/18.76
r_{bend}/m	5820	7450
L/m	0.780	0.712
A_{CCD}/mm	16	13

formation of visible clumps in the initial reagent mixture that are not easily eliminated by the gentle RAM treatment. This hygroscopic nature also hindered our attempts to explore Au NP synthesis in the RAM using a milling ball, and our attempts led to immediate caking at the high RAM intensities.

The RAM is evidently an exciting platform for the development and scale-up of nanoparticle synthesis. While rheological problems precluded a detailed study of the chemistry in this case, the RAM-driven BUMS of Au NPs clearly demonstrates that TRIS-DXAS offers a transformative step in the development of x-ray spectroscopy for mechanochemical investigations.

C. Mechanochemical synthesis of ZIF-8

The synthesis of ZIF-8 by resonant acoustic mixing (RAM) has been previously reported,[26] although the kinetics of the reaction have only been investigated in a ball mill.[15,36] Our initial investigations for TRIS monitoring of the RAM synthesis of ZIF-8 followed the successful RAM conditions outlined in Ref. 26 using an acceleration of 95 g. At this acceleration, we experienced significant sedimentation of the material within seconds of the reaction, reducing the amount of powder passing through the x-ray beam and thereby making it impossible to monitor the reaction. The issue of powder sedimentation was significantly reduced by conducting

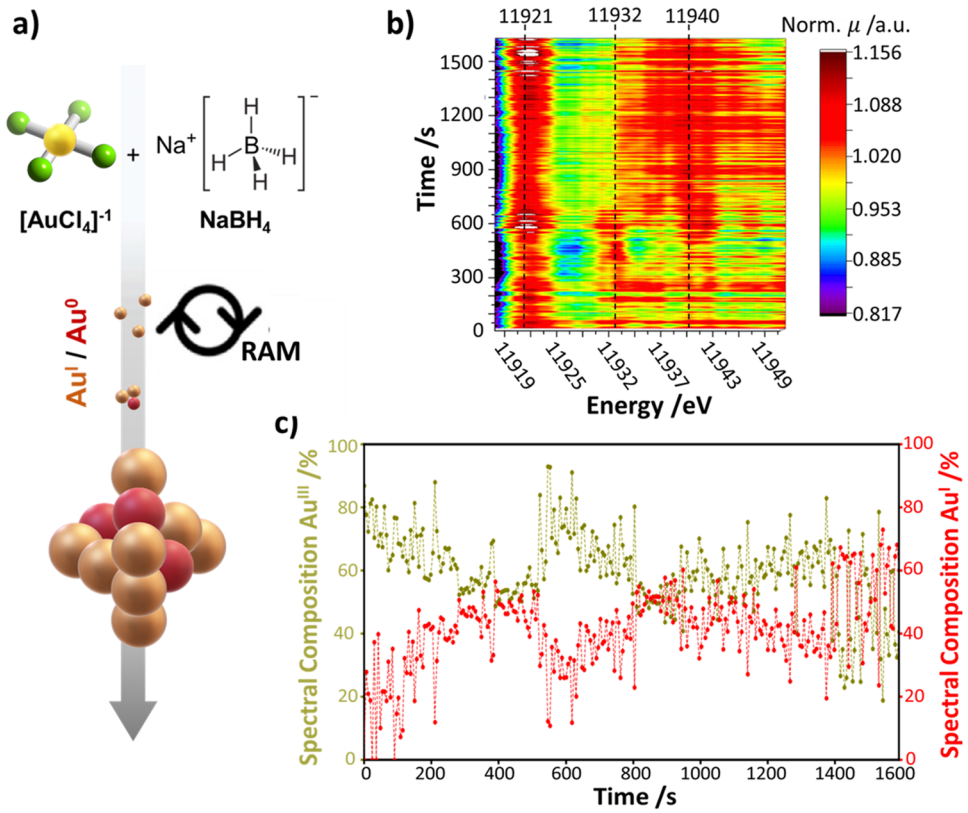

FIG. 2. Monitoring RAM synthesis of Au using TRIS-DXAS. (a) Reaction scheme for the BUMS synthesis of Au nanoparticles with $NaBH_4$ by RAM. (b) A heatmap showing the evolution of the TRIS-DXAS spectra over the course of Au reduction during RAM. Specific features are indicated that correspond to Au^{III} (11 921 eV) and Au^{I} (both 11 932 and 11 940 eV); see Appendix D. (c) A quantitative analysis of the TRIS-DXAS data showing the conversion of Au^{III} (gold) to Au^{I} (red).

the reaction at 80 g, Appendix C, which allowed us to successfully measure the Zn K-edge in the reaction mixture. Unfortunately, at this frequency, all of the powder "clustered" (presumably in an acoustic node) directly in the beam path. Thus, while an excellent edge jump was observed as a result of the clustering, see Appendix C, the fine spectral details that are needed to follow ZIF-8 formation (i.e., splitting of the white line) were not visible, precluding further study of the reaction. It is therefore evident that, as for TRIS-XRD,[36] dedicated work is needed to optimize RAM conditions (including jar design and powder loading) for TRIS-DXAS measurements.

Fortunately, we were able to bypass these issues with powder behavior by further reducing the acceleration to 60 g, allowing the first TRIS-DXAS study of RAM ZIF-8 synthesis, Fig. 3. The formation of ZIF-8 from ZnO and 2-methylimidazole is clearly visible by the splitting of the Zn^{II} white line (9.670 keV) into two maxima, one at ~9.665 keV and the second at ~9.673 keV, Fig. 3. In contrast to the ball milling synthesis of ZIF-8, which occurs within seconds as seen by TRIS-XRD,[15,36] the RAM synthesis of ZIF-8 is very gradual at 60 g, occurring gradually over ~400–500 s. Moreover, despite the lack of milling media, the formation of ZIF-8 appears to occur continuously, suggesting the formation of new reactive contacts occurs readily under the gentle RAM conditions. This macrokinetic behavior is consistent with early TRIS-XRD studies of RAM cocrystallization.[25] However, we note that at this low intensity of mixing at 60 g acceleration, the reaction does not proceed to completion, instead reaching a notable plateau (at ~80%), despite prolonged RAM treatment. This does suggest there may be issues with mixing (e.g., comminution or refreshing particle surfaces[38]) when conducting RAM reactions of hard inorganic compounds at low accelerations. Regardless, the results are a promising demonstration that reactions conducted by RAM can be followed with exceptional (2 s) time resolution by TRIS-DXAS.

Most of the current interest in mechanochemistry involves the use of various ball mills, which contain sizable (typically 3–8 mm) stainless steel balls. We therefore aimed to further explore whether our TRIS-DXAS approach was amenable to similar ball milling conditions by adding a 3 mm stainless steel milling ball to the RAM vessel, effectively converting the RAM into a ball mill. For convenience, we call this a RAM ball mill (RAM-bm). Under these conditions, the synthesis of ZIF-8 was significantly faster, Fig. 3. In fact, even the exceptional time resolution of our setup (2 s data acquisition) was insufficient to catch the earliest stages of ZIF-8 formation, Fig. 3(c). As RAM-bm continues, there is a very clear separation of the Zn^{II} white line into two maxima until the reaction achieves full conversion in 120 s. This further suggests that more intense mechanochemical conditions are required to facilitate the mixing of hard inorganic solids. However, we do note that the edge jump decreases slightly over the course of our RAM-bm experiment, which indicates that some of the material does become caked outside the beam path over the course of the experiment. Such effects are well-known and common in TRIS analysis[5,36,37] and represent a significant hurdle to further developing TRIS methodologies.

We stress that this entire reaction occurs in ~10% of the acquisition time of our previous TRIS-XAS setup, with its successful

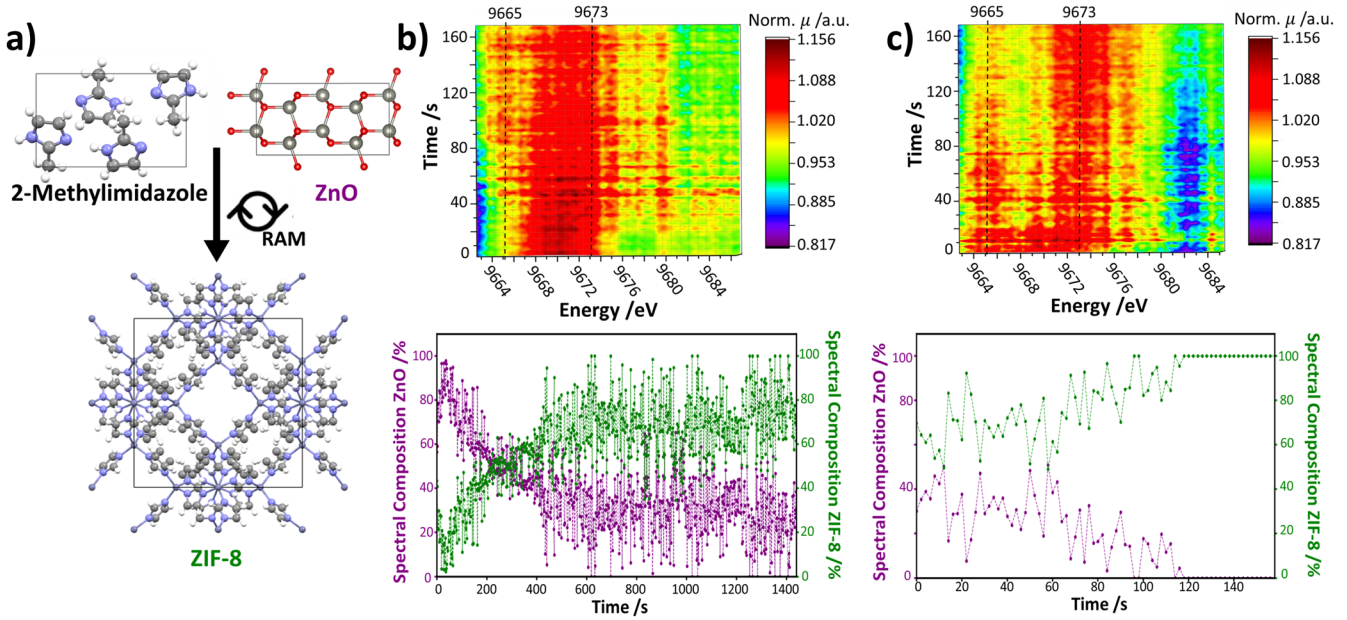

FIG. 3. Monitoring RAM synthesis of ZIF-8 using TRIS-DXAS. (a) Reaction scheme for the formation of ZIF-8 from crystalline 2-methylimidazole and ZnO by RAM, with mechanochemical symbol as suggested by.[1] (b) RAM synthesis of ZIF-8 at 60 g (top), alongside quantitative phase analysis via least squares fitting (bottom). (c) RAM synthesis of ZIF-8 at 60 G, with the addition of one 3 mm diameter stainless steel milling ball (top), alongside quantitative phase analysis via. Note that the decrease in absolute intensity in (c) is presumably due to the caking of material and hence a reduction in the amount of absorbing material. Specific features corresponding to ZIF-8 (9665 eV) and ZnO (9673 eV) are indicated.

monitoring representing an immense improvement on methodology. Moreover, we note that mechanochemical reactions of this speed are still difficult to monitor by state-of-the-art TRIS-XRD methods, placing our technique on par with these diffraction-based approaches. Given this immense improvement, placing our TRIS-DXAS method on par with TRIS-XRD, we are certain this technique will become an essential component of the mechanochemistry toolbox, allowing access not just to crystal structure but, for the first time, electronic structure information.

IV. CONCLUSION

We here demonstrate the first successful monitoring of mechanochemical reactions using x-ray absorption spectroscopy (XAS) with time resolution (2 s) that is competitive with state-of-the-art *in situ* monitoring methods such as powder x-ray diffraction. This has been achieved using a dispersive x-ray absorption spectrometer setup. By following the kinetics of Au^{III} reduction and of ZIF-8 synthesis, both under resonant acoustic mixing (RAM) conditions, we demonstrate that XAS offers a powerful and complementary addition to the toolbox of time-resolved *in situ* (TRIS) methods that are available for mechanochemical research. Moreover, we demonstrate that our TRIS-XAS approach is also suitable to follow ball milling transformations, thereby opening its applicability beyond ball-free RAM. With a unique ability to follow changes in the electronic structure of materials without the limitation of capturing only crystalline materials, TRIS-XAS opens the door to exciting and detailed views of mechanochemical reactions that have been so far unobservable.

ACKNOWLEDGMENTS

Experiments were performed at the BAM*line* at the BESSY-II storage ring (Helmholtz Center Berlin). We thank the Helmholtz-Zentrum Berlin für Materialien und Energie for the allocation of synchrotron radiation beamtime. The authors thank Ms. B Röder for manufacturing jars suitable for *in situ* analysis. P.F.M. de Oliveira thanks Sao Paulo Research Foundation (FAPESP Grant Nos. 2020/14955-6 and 2021/12899-4) for funding. This research used facilities of the Brazilian Synchrotron Light Laboratory (LNLS), part of the Brazilian Center for Research in Energy and Materials (CNPEM), a private, non-profit organization under the supervision of the Brazilian Ministry for Science, Technology, and Innovation (MCTI). The CARNAUBA beamline staff is acknowledged for their assistance during the experiments 20220095.

AUTHOR DECLARATIONS

Conflict of Interest

The authors have no conflicts to disclose.

Author Contributions

Ana Guilherme Buzanich: Conceptualization (equal); Formal analysis (lead); Investigation (equal); Methodology (equal); Writing – original draft (equal). **C. Tufan Cakir**: Investigation (supporting); Software (supporting). **Martin Radtke**: Methodology (supporting); Writing – review & editing (supporting). **M. Bilal Haider**: Investigation (supporting); Writing – review & editing (supporting). **Franziska Emmerling**: Resources (equal); Writing – review & editing (equal). **Paulo F. M. de Oliveira**: Conceptualization (supporting); Investigation (supporting); Writing – review & editing (equal). **Adam A. L. Michalchuk**: Conceptualization (lead); Formal analysis (equal); Investigation (lead); Methodology (equal); Supervision (lead); Writing – original draft (lead).

DATA AVAILABILITY

The data that support the findings of this study are available within the article and corresponding author upon reasonable request.

APPENDIX A: XAS STANDARDS

Quantitative analysis (see Appendix B) of our TRIS-DXAS data requires a comparison to high-quality reference XAS spectra for each reagent involved. For all cases, these reference spectra were collected using well-defined standards, measured using a conventional transmission setup at the CARNAUBA beamline (Sirius, Brazil), Fig. 8. Standards for the BUMS Au NP reaction include an Au(0) foil and a pellet (in polyvinylpyrrolidone to avoid sample deliquescence) of $HAuCl_4$ for Au^{III}. AuCl was used as a standard for Au^{I}. The sample of AuCl was prepared in a glove box under an Ar atmosphere to avoid disproportionation. The AuCl powder was closed in Kapton tape and measured immediately after removal from the glove box. For the ZIF-8 reaction, pellets (in BN) of ZnO and ZIF-8 were used for standard measurements, Fig. 8.

APPENDIX B: TRIS DXAS DATA PROCESSING

TRIS DXAS data were acquired as shown in Fig. 1. X rays are converted into visible light using a fluorescence screen in front of the CCD. Images were collected with 2 s time resolution for both reactions. At the end of the reaction, a picture of the I_0 is taken by collecting the CCD image without a sample being placed in the beam. For each dataset, the CCD image of the sample (I_1) is divided by the I_0 image, in the same manner as for standard XAS measurements. This follows the known Beer–Lambert law. To generate an XAS spectrum from the CCD image, the CCD pixel positions are converted into energy using a calibration function. We generate this calibration for each absorption edge by scanning an incident monochromatic beam in 10 eV steps with an Au or Zn metal reference foil. A linear relationship between pixel and energy was obtained for both Au and Zn, according to B1 and B2, respectively,

$$y(\mathrm{eV}) = 11\,732.37 + 0.144 \times x(pixel), \tag{B1}$$

$$y(\mathrm{eV}) = 9423.65 + 0.159 \times x(pixel). \tag{B2}$$

The data are processed following standard protocols. This includes normalization of the data to the pre-edge range, which is fit with a linear function, and to the post-edge range, which is fit with a second-order polynomial function. In our work, this normalization procedure was performed using the open-source library xraylarch for Python (v0.9.65).[27] A total of 800 spectra were collected for the Au reaction, Figs. 4(a) and 4(b). This corresponds to a total reaction

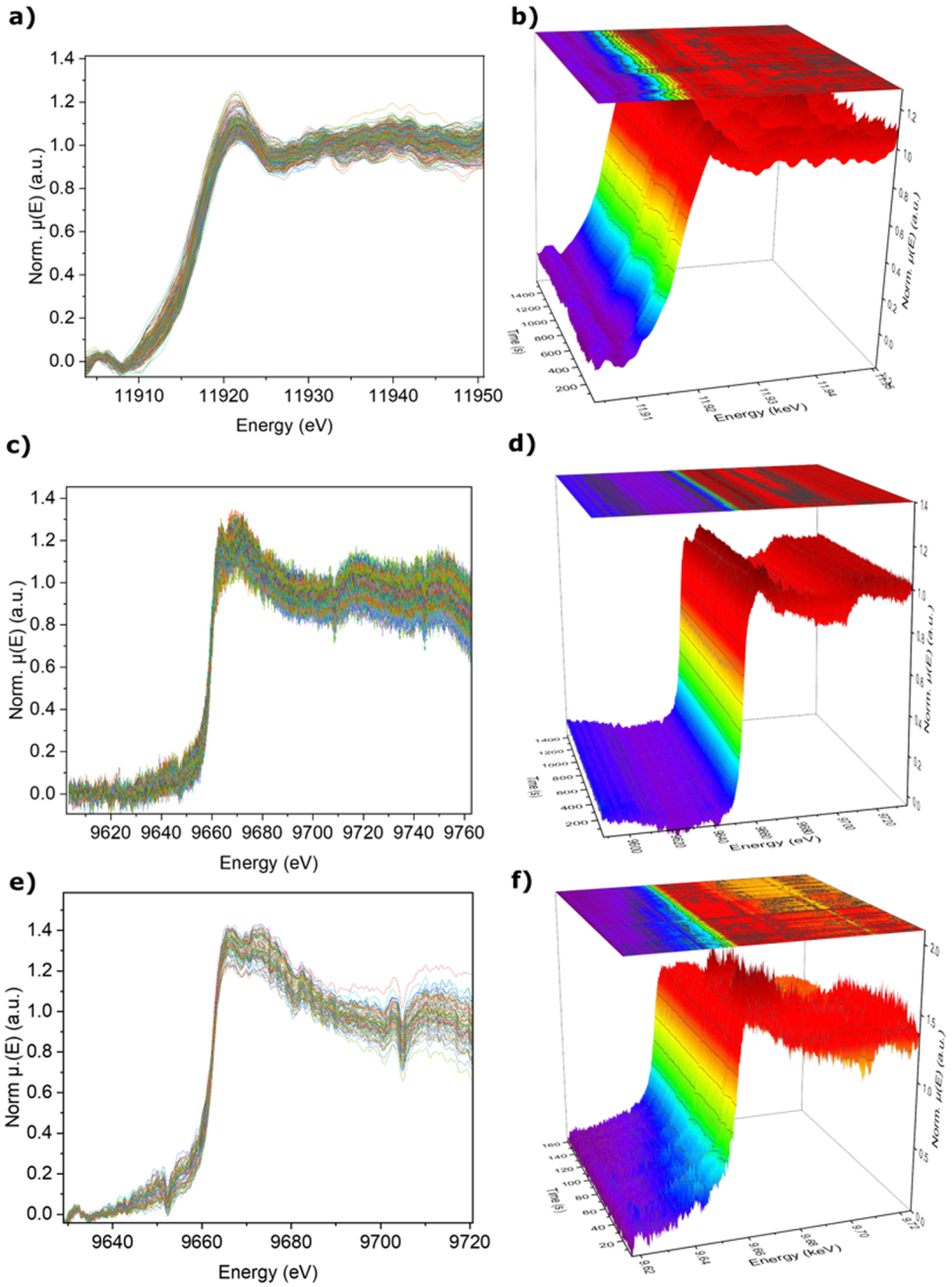

FIG. 4. 2D and 3D plots of normalized XANES spectra of the whole reaction for gold (a) and (b), and for zinc (c) and (d) without milling media and (e) and (f) with milling media. The plots in (a) and (b) correspond to a time resolution of 6 s, and the plots in (c)–(f) correspond to a time resolution of 2 s.

time of 26 minutes. For the RAM synthesis of ZIF-8, Figs. 4(c) and 4(d), 720 spectra were acquired from a 24 min. reaction. In contrast, when a 3 mm milling ball was added to the reaction vile, the reaction reached completion after only 3 min (82 spectra), Figs. 4(e) and 4(f). The whole ZIF-8 synthesis without milling media is displayed in Fig. 5.

For all reactions, quantification was performed by least squares fitting (LS) using a Gaussian width 2 filtering to smooth the curves, Fig. 6. This minor Gaussian filtering ensured that the absorption features were not affected. LS fitting was performed with the Graphical User Interface XASViewer from Larch, using the standards mentioned in A. For the Au reaction, the fit was performed using data between 11907 and 11950 eV; for the ZIF-8 reaction, the fit was performed for data between 9660 and 9680 eV. In all cases, the best fit with the lowest χ^2 was used, where an uncertainty of ~5% should be taken for all datasets.

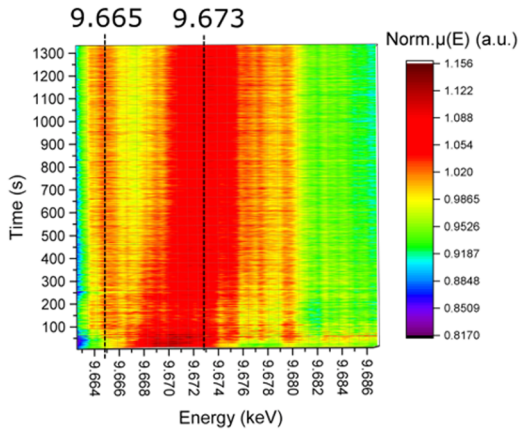

FIG. 5. TRIS-DXAS data for the entire RAM synthesis of ZIF-8 at 60 g.

APPENDIX C: EFFECTS OF RAM ACCELERATION ON DATA QUALITY

In the case of the ZIF-8 reaction, we observed that the acceleration was affecting the data quality, specifically at 80 g. Figure 7 shows a comparison between 60 and 80 g of non-normalized spectra, at the beginning and end of each reaction. With non-normalized data, we can directly see the effects of the thickness of the sample. The higher the absorption jump (ratio between before and after the absorption edge), the thicker the sample. In the case of 80 g, this is clearly thicker, which means a higher amount of powder was in the beam. This hinders resolving the absorption features, as shown. The features of both ZnO and ZIF-8 are not visible at 80 g.

APPENDIX D: COMPARING *IN SITU* AND EX SITU SPECTRA

As a qualitative evaluation of the reaction evolution and full or partial completion, Fig. 8 shows a comparison between the beginning and end of each reaction with the respective reference XAS spectra. Assessing the spectra of two point of the Au reaction, it is clear the partial conversion from Au^{III} to Au^{I}. Although the first

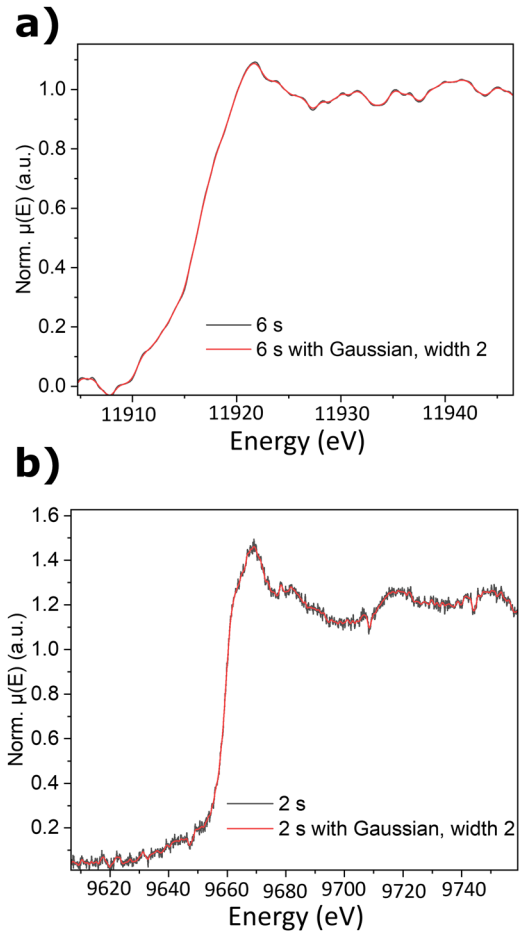

FIG. 6. Effect of Gaussian width on the quality of TRIS-DXAS data for (a) the Au reaction and (b) the synthesis of ZIF-8.

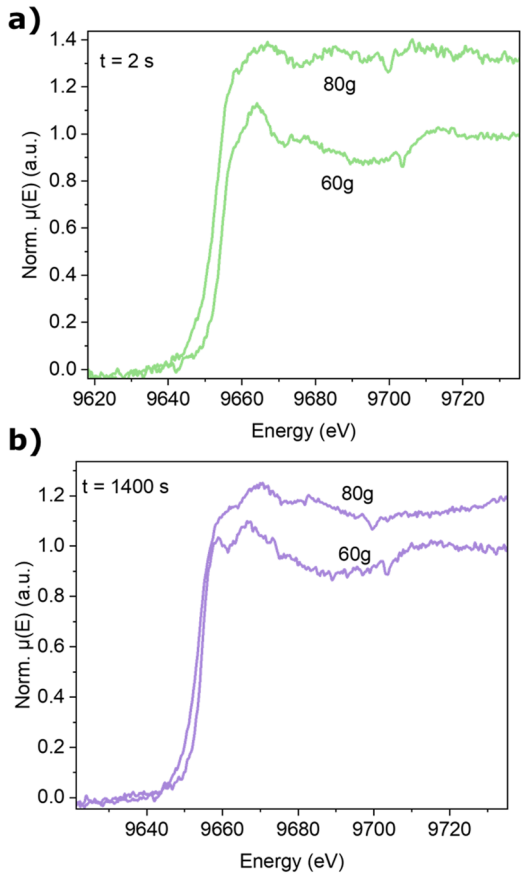

FIG. 7. Non-normalized XANES spectra of the ZIF-8 reaction at 60 and 80 g (a) at the beginning (2 s) and (b) at the end (1400 s) of the reaction.

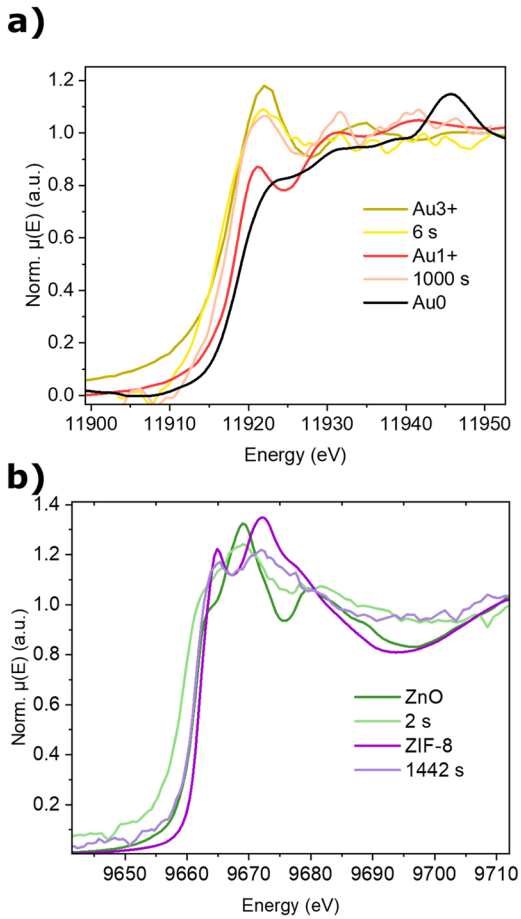

FIG. 8. Comparison of XAS spectra measured *in situ* at the beginning and end of each reaction for (a) gold and (b) zinc. The XAS spectra of the respective references are plotted accordingly.

absorption maximum at 11922 eV is still strongly pronounced at the end of the reaction, the characteristic maxima of Au^{I} at 11932.7 and 11940 eV are clearly visible. As for the Zn spectra, they show even stronger signs of the conversion from ZnO, where one absorption maximum is visible, to ZIF-8, with a splitting into two maxima.

REFERENCES

[1]A. A. L. Michalchuk, E. V. Boldyreva, A. M. Belenguer, F. Emmerling, and V. V. Boldyrev, "Tribochemistry, mechanical alloying, mechanochemistry: What is in a name?" Front. Chem. **9**, 359 (2021).

[2]V. V. Boldyrev, "Mechanochemistry and mechanical activation of solids," Russ. Chem. Rev. **75**, 177–189 (2006).

[3]M. J. Cliffe, C. Mottillo, R. S. Stein, D.-K. Bučar, and T. Friščić, "Accelerated aging: A low energy, solvent-free alternative to solvothermal and mechanochemical synthesis of metal–organic materials," Chem. Sci. **3**, 2495 (2012).

[4]T. Stolar, L. Batzdorf, S. Lukin, D. Žilić, C. Motillo, T. Friščić, F. Emmerling, I. Halasz, and K. Užarević, "In situ monitoring of the mechanosynthesis of the archetypal metal–organic framework HKUST-1: Effect of liquid additives on the milling reactivity," Inorg. Chem. **56**, 6599–6608 (2017).

[5]A. A. L. Michalchuk, I. A. Tumanov, S. Konar, S. A. J. Kimber, C. R. Pulham, and E. V. Boldyreva, "Challenges of mechanochemistry: Is in situ real-time quantitative phase analysis always reliable? A case study of organic salt formation," Adv. Sci. **4**, 1700132 (2017).

[6]A. A. L. Michalchuk and F. Emmerling, "Time-resolved in situ monitoring of mechanochemical reactions," Angew. Chem., Int. Ed. **61**, e202117270 (2022).

[7]A. A. L. Michalchuk, A. Kabelitz, and F. Emmerling, "Monitoring mechanochemical processes in situ and in real time," *Nontraditional Activation Methods in Green and Sustainable Applications* (Elsevier, 2021), pp. 369–419.

[8]J. Beamish-Cook, K. Shankland, C. A. Murray, and P. Vaqueiro, "Insights into the mechanochemical synthesis of MOF-74," Cryst. Growth Des. **21**, 3047–3055 (2021).

[9]H. Kulla, A. A. L. Michalchuk, and F. Emmerling, "Manipulating the dynamics of mechanochemical ternary cocrystal formation," Chem. Commun. **55**, 9793–9796 (2019).

[10]S. Lukin, L. S. Germann, T. Friščić, and I. Halasz, "Toward mechanistic understanding of mechanochemical reactions using real-time *in situ* monitoring," Acc. Chem. Res. **55**, 1262–1277 (2022).

[11]T. Friščić, I. Halasz, P. J. Beldon, A. M. Belenguer, F. Adams, S. A. Kimber, V. Honkimäki, and R. E. Dinnebier, "Real-time and *in situ* monitoring of mechanochemical milling reactions," Nat. Chem. **5**, 66–73 (2013).

[12]D. Gracin, V. Štrukil, T. Friščić, I. Halasz, and K. Užarević, "Laboratory real-time and in situ monitoring of mechanochemical milling reactions by Raman spectroscopy," Angew. Chem., Int. Ed. **53**, 6193–6197 (2014).

[13]L. Batzdorf, F. Fischer, M. Wilke, K.-J. Wenzel, and F. Emmerling, "Direct in situ investigation of milling reactions using combined x-ray diffraction and Raman spectroscopy," Angew. Chem., Int. Ed. **54**, 1799–1802 (2015).

[14]S. Haferkamp, A. Paul, A. A. L. Michalchuk, and F. Emmerling, "Unexpected polymorphism during a catalyzed mechanochemical Knoevenagel condensation," Beilstein J. Org. Chem. **15**, 1141–1148 (2019).

[15]H. Kulla, S. Haferkamp, I. Akhmetova, M. Röllig, C. Maierhofer, K. Rademann, and F. Emmerling, "In situ investigations of mechanochemical one-pot syntheses," Angew. Chem., Int. Ed. **57**, 5930–5933 (2018).

[16]N. Cindro, M. Tireli, B. Karadeniz, T. Mrla, and K. Užarević, "Investigations of thermally controlled mechanochemical milling reactions," ACS Sustainable Chem. Eng. **7**, 16301–16309 (2019).

[17]J. G. Schiffmann, F. Emmerling, I. C. B. Martins, and L. Van Wüllen, "*In-situ* reaction monitoring of a mechanochemical ball mill reaction with solid state NMR," Solid State Nucl. Magn. Reson. **109**, 101687 (2020).

[18]C. Leroy, S. Mittelette, G. Félix, N. Fabregue, J. Špačková, P. Gaveau, T.-X. Métro, and D. Laurencin, "*Operando* acoustic analysis: A valuable method for investigating reaction mechanisms in mechanochemistry," Chem. Sci. **13**, 6328–6334 (2022).

[19]S. Grätz, D. Beyer, V. Tkachova, S. Hellmann, R. Berger, X. Feng, and L. Borchardt, "The mechanochemical Scholl reaction—A solvent-free and versatile graphitization tool," Chem. Commun. **54**, 5307–5310 (2018).

[20]I. Brekalo, W. Yuan, C. Mottillo, Y. Lu, Y. Zhang, J. Casaban, K. T. Holman, S. L. James, F. Duarte, P. A. Williams, K. D. M. Harris, and T. Friščić, "Manometric real-time studies of the mechanochemical synthesis of zeolitic imidazolate frameworks," Chem. Sci. **11**, 2141–2147 (2020).

[21]P. F. M. de Oliveira, A. A. L. Michalchuk, A. G. Buzanich, R. Bienert, R. M. Torresi, P. H. C. Camargo, and F. Emmerling, "Tandem x-ray absorption spectroscopy and scattering for *in situ* time-resolved monitoring of gold nanoparticle mechanosynthesis," Chem. Commun. **56**, 10329 (2020).

[22]A. G. Buzanich, M. Radtke, U. Reinholz, H. Riesemeier, and F. Emmerling, "Time- and spatial-resolved XAFS spectroscopy in a single shot: New analytical possibilities for *in situ* material characterization," J. Synchrotron Radiat. **23**, 769–776 (2016).

[23]A. Iglesias-Juez, A. Martínez-Arias, M. A. Newton, S. G. Fiddy, and M. Fernández-García, "Redox behaviour of Pd-based TWCs under dynamic conditions: Analysis using dispersive XAS and mass spectrometry," Chem. Commun. **2005**, 4092–4094 .

[24]S. R. Anderson, D. J. am Ende, J. S. Salan, and P. Samuels, "Preparation of an energetic-energetic cocrystal using resonant acoustic mixing," Propellants, Explos., Pyrotech. **39**, 637–640 (2014).
[25]A. A. L. Michalchuk, K. S. Hope, S. R. Kennedy, M. V. Blanco, E. V. Boldyreva, and C. R. Pulham, "Ball-free mechanochemistry: *In situ* real-time monitoring of pharmaceutical co-crystal formation by resonant acoustic mixing," Chem. Commun. **54**, 4033–4036 (2018).
[26]H. M. Titi, J.-L. Do, A. J. Howarth, K. Nagapudi, and T. Friščić, "Simple, scalable mechanosynthesis of metal–organic frameworks using liquid-assisted resonant acoustic mixing (LA-RAM)," Chem. Sci. **11**, 7578–7584 (2020).
[27]M. Newville, "Larch: An analysis package for XAFS and related spectroscopies," J. Phys.: Conf. Ser. **430**, 012007 (2013).
[28]A. Kulow, S. Witte, S. Beyer, A. Guilherme Buzanich, M. Radtke, U. Reinholz, H. Riesemeier, and C. Streli, "A new experimental setup for time- and laterally-resolved x-ray absorption fine structure spectroscopy in a 'single shot,'" J. Anal. At. Spectrom. **34**, 239–246 (2019).
[29]M. J. Rak, N. K. Saadé, T. Friščić, and A. Moores, "Mechanosynthesis of ultra-small monodisperse amine-stabilized gold nanoparticles with controllable size," Green Chem. **16**, 86–89 (2014).
[30]M. J. Rak, T. Friščić, and A. Moores, "Mechanochemical synthesis of Au, Pd, Ru and Re nanoparticles with lignin as a bio-based reducing agent and stabilizing matrix," Faraday Discuss. **170**, 155–167 (2014).
[31]P. F. M. De Oliveira, A. A. L. Michalchuk, J. Marquardt, T. Feiler, C. Prinz, R. M. Torresi, P. H. C. Camargo, and F. Emmerling, "Investigating the role of reducing agents on mechanosynthesis of Au nanoparticles," CrystEngComm **22**, 6261–6267 (2020).
[32]P. F. M. de Oliveira, R. M. Torresi, F. Emmerling, and P. H. C. Camargo, "Challenges and opportunities in the bottom-up mechanochemical synthesis of noble metal nanoparticles," J. Mater. Chem. A **8**, 16114–16141 (2020).
[33]L. Yang, A. Moores, T. Friščić, and N. Provatas, "Thermodynamics model for mechanochemical synthesis of gold nanoparticles: Implications for solvent-free nanoparticle production," ACS Appl. Nano Mater. **4**, 1886–1897 (2021).
[34]M. Ferguson, A. J. Richard, J. Valdez, B. G. Fiss, H. M. Titi, N. Provatas, T. Friščić, and A. Moores, "Direct observation by high resolution transmission electron microscopy of gold(III) particle transformation during aging reduction reaction," Faraday Discuss. (published online) (2022).
[35]B. P. Khanal and E. R. Zubarev, "Gram-scale synthesis of isolated monodisperse gold nanorods," Chem. Eur. J. **25**, 1595–1600 (2019).
[36]G. I. Lampronti, A. A. L. Michalchuk, P. P. Mazzeo, A. Belenguer, J. K. M. Sanders, A. Bacchi, and F. Emmerling, "Changing the game of time resolved x-ray diffraction on the mechanochemistry playground by downsizing," Nat. Commun. **12**, 6134 (2021).
[37]A. A. L. Michalchuk, I. A. Tumanov, and E. V. Boldyreva, "Complexities of mechanochemistry: Elucidation of processes occurring in mechanical activators via implementation of a simple organic system," CrystEngComm **15**, 6403 (2013).
[38]K. Linberg, P. Szymoniak, A. Schönhals, F. Emmerling, and A. A. L. Michalchuk, "The origin of delayed polymorphism in molecular crystals under mechanochemical conditions," ChemRxiv:10.26434/chemrxiv-2022-04jdf (2022).